

MASSIVE BLACK HOLE SEEDS

JOHN A. REGAN¹ AND MARTA VOLONTERI²

¹Centre for Astrophysics and Space Science Maynooth, Department of Physics, Maynooth University, Maynooth, Ireland

²Institut d'Astrophysique de Paris, Sorbonne Université, CNRS, UMR 7095, 98 bis bd Arago, 75014 Paris, France

Version September 4, 2024

ABSTRACT

The pathway(s) to seeding the massive black holes (MBHs) that exist at the heart of galaxies in the present and distant Universe remains an unsolved problem. Here we categorise, describe and quantitatively discuss the formation pathways of both *light* and *heavy* seeds. We emphasise that the most recent computational models suggest that rather than a bimodal-like mass spectrum between *light* and *heavy* seeds with *light* at one end and *heavy* at the other that instead a continuum exists. *Light* seeds being more ubiquitous and the heavier seeds becoming less and less abundant due the rarer environmental conditions required for their formation. We therefore examine the different mechanisms that give rise to different seed mass spectrums. We show how and why the mechanisms that produce the *heaviest* seeds are also among the rarest events in the Universe and are hence extremely unlikely to be the seeds for the vast majority of the MBH population. We quantify, within the limits of the current large uncertainties in the seeding processes, the expected number densities of the seed mass spectrum. We argue that *light* seeds must be at least 10^3 to 10^5 times more numerous than *heavy* seeds to explain the MBH population as a whole. Based on our current understanding of the seed population this makes *heavy* seeds ($M_{\text{seed}} > 10^3 M_{\odot}$) a significantly more likely pathway given that *heavy* seeds have an abundance pattern than is close to and likely in excess of 10^{-4} compared to *light* seeds. Finally, we examine the current state-of-the-art in numerical calculations and recent observations and plot a path forward for near-future advances in both domains.

1. INTRODUCTION

Massive black holes (MBHs) with masses up to $10^{10} M_{\odot}$ exist at the centre of most, perhaps all, massive galaxies. The ongoing challenge in the field is to understand the origin of the central MBHs. Up until recently the most distant MBHs discovered were quasars with masses up to $10^9 M_{\odot}$ observed at redshifts just beyond seven (approximately 700 Myr after the Big Bang) (Fan, Carilli & Keating 2006; Mortlock et al. 2011; Venemans et al. 2013, 2015; Bañados et al. 2018; Yang et al. 2021; Wang et al. 2021). However, while these observations strongly indicate that the seeds for MBHs must form in the early Universe they offer little insight into their origin, as the initial conditions within which the seed black hole formed have long since been erased and the black hole itself contains no signature of that event.

More recently, observations with JWST have uncovered MBHs with masses in the range $10^6 M_{\odot}$ to $10^8 M_{\odot}$ (Kovács et al. 2024; Maiolino et al. 2024b; Larson et al. 2023; Bogdán et al. 2023; Matthee et al. 2024; Greene et al. 2024) at even higher redshifts. These MBH masses are lower than the high-z quasar masses previously detected but the galaxies within which these “JWST-quasars” have been detected likely represent the tip of the iceberg at this time in terms of both halo and stellar masses (Boylan-Kolchin 2023; Juodžbalis et al. 2024; Li et al. 2024). Nonetheless, with inferred masses down as low as $5 \times 10^6 M_{\odot}$ (Maiolino et al. 2024b) these observations set an upper limit to the seed masses of this population of MBHs at the very least. The number density of these MBH host galaxies is currently unclear with

potentially significant evolution of the central black hole following seeding. If we assume that current candidate AGN being observed by JWST are indeed true AGN then the number densities could be of the order 10^{-4} to $10^{-3} \text{ cMpc}^{-3}$ (Matthee et al. 2024; Greene et al. 2024; Scholtz et al. 2023). *The goal of this paper is to highlight what the current state-of-the-art in MBH seeding is, to identify challenges in the current models and to plot a path forward in terms of reconciling current theoretical models with observational data.*

The models for the astrophysical formation of MBH seeds can be loosely broken down into *light* and *heavy* seed models. Here, we define a *light* seed as any seed black hole with a mass less than $1000 M_{\odot}$ and a *heavy* seed as any seed black hole with an initial mass in excess of $1000 M_{\odot}$. A key challenge is then to understand what the mass spectrum and number densities of MBH seeds is and to understand the growth prospects of the seeds. We illustrate this challenge to the field in Figure 1.

The crucial question for the black hole population is “Does the entire black hole mass spectrum originate from stellar mass black holes with characteristic masses of approximately $40 M_{\odot}$ and a tail to higher and lower masses, which grow through accretion and mergers?” This would imply a continuum from stellar black holes to MBHs, with a single origin for all of them. Or is another channel required to populate the MBH mass spectrum? Depending on the mass distribution of this channel then this channel will, if it exists, give rise to an additional peak in the mass spectrum of black holes. Tantalisingly this peak could, in theory, be detected by future gravitational wave observations (Sesana, Volonteri & Haardt 2007, 2009).

*E-mail:john.regan@mu.ie

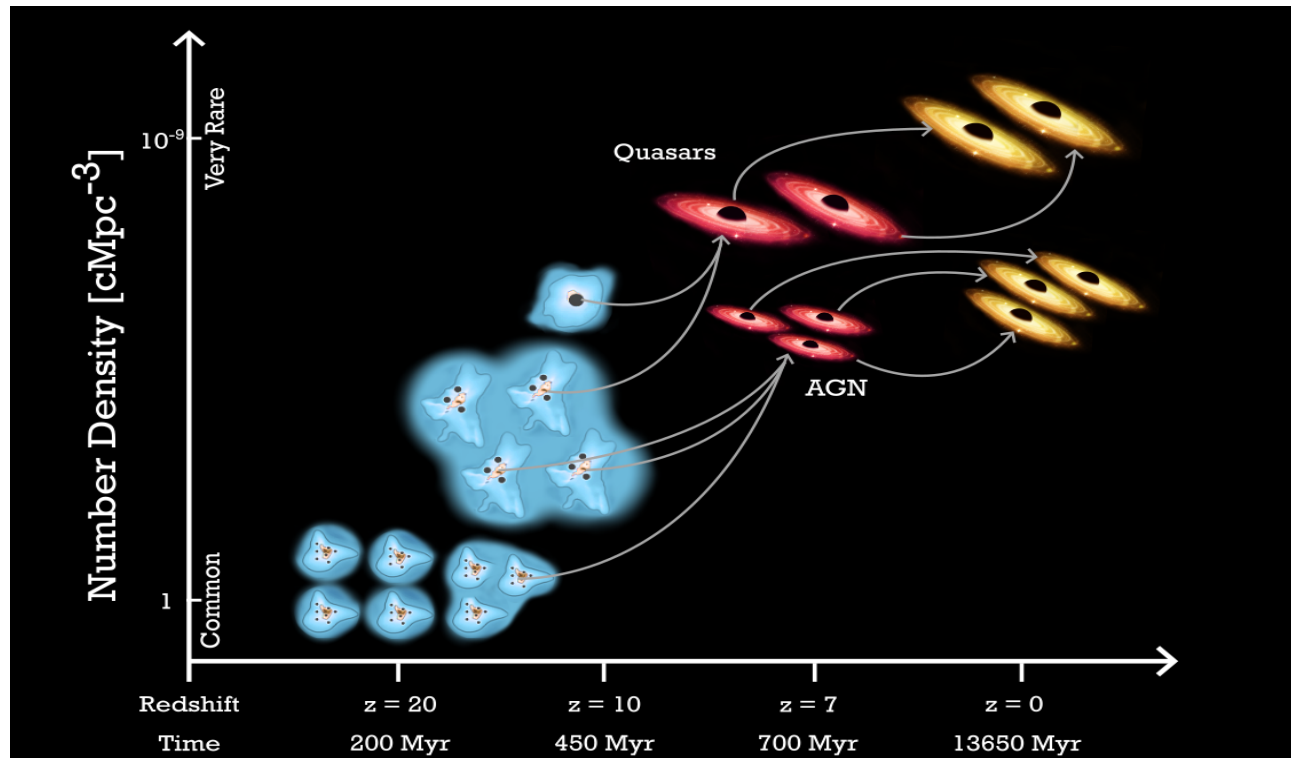


FIG. 1.— Schematic showing the Number Density (rarity, y-axis) versus Time and Redshift. *Light* seeds can form in ‘normal’ galaxies with relative ubiquity in the early universe with number densities of the order of 1 cMpc^{-3} at redshifts between $z = 20$ and $z = 10$. However, their (initially) small masses make them unlikely to be the progenitors for all of the ‘JWST’ AGN or the high- z quasar population. On the other hand forming heavier seeds requires rarer environmental conditions and number densities varying from 10^{-1} to $10^{-5} \text{ cMpc}^{-3}$ (perhaps lower) but their initially heavier masses can facilitate more rapid growth potentially explaining the early MBH population as well as the high- z quasar population.

The simplest case is to assume that the seeds are indeed *light* and that they originated from the remnants of the first stars (e.g. [Madau & Rees 2001](#)). However, significant challenges to *light* seed growth exist and we will address this question in detail in §2.

Alternative routes to MBH formation may be through either a dynamical runaway pathway where either stellar collisions and/or black hole mergers result in a *heavy* seed. Another possibility is a near monolithic collapse, or at least reduced fragmentation of a massive gas cloud, resulting in the formation of a supermassive star (SMS). Both of these mechanisms create a *heavy* seed with masses in excess of approximately $10^3 M_{\odot}$ and in some cases possibly up to $10^5 M_{\odot}$. We will address these questions and gauge their possible number density in §3. We begin by first briefly reviewing the *light* seed model and then the *heavy* seed model. More in-depth reviews of the mechanisms can be found in reviews by [Latif & Ferrara \(2016\)](#); [Woods et al. \(2017\)](#); [Inayoshi, Visbal & Haiman \(2020\)](#); [Volonteri, Habouzit & Colpi \(2021\)](#). Additional mechanisms, which we will not consider in this paper, include supermassive stars fuelled by dark matter annihilation (e.g. [Spolyar, Freese & Gondolo 2008](#); [Feng, Yu & Zhong 2021](#); [Singh, Monaco & Tan 2023](#)) or primordial black holes (e.g., [Carr & Silk 2018](#); [Hasinger 2020](#)). We do not consider these mechanisms here as there is still considerable uncertainty in their formation pathway and their possible number densities. However, continued research into these mechanisms is warranted given the outstanding questions over the mainstream pathways, as we now discuss, as well as the ability of “non-standard”

dark matter to potentially solve other dynamical hurdles (e.g. [Alonso-Álvarez, Cline & Dewar 2024](#)).

2. LIGHT SEEDS AS THE ORIGIN OF ALL MBHS

While this is indeed the simplest explanation there are significant challenges in growing *light* seeds in order to explain the entire MBH mass spectrum. The problem is particularly acute when attempting to use *light* seed growth to explain the appearance of MBHs at $z \gtrsim 7$. In order to achieve such growth the seed black holes would need to grow, uninterrupted, at the Eddington rate (under the assumption that *light* seeds form from the first or second generation of stars). The Eddington accretion rate is given by

$$M(t) = M_0 \exp\left(\frac{1 - \epsilon_r}{\epsilon_r} \frac{t}{t_{\text{Edd}}}\right), \quad (1)$$

where $t_{\text{Edd}} = 0.45 \text{ Gyr}$ and ϵ_r is the radiative efficiency. For a “standard” radiative efficiency of $\epsilon_r \sim 0.1$ and a black hole seed mass of $M_0 = 10^2 M_{\odot}$, it takes nearly 1 Gyr to grow from $M(0)$ up to $\sim 10^9 M_{\odot}$. While therefore in principle marginally allowable with current observational constraints the growth must continue at the Eddington rate all the way up to the maximum mass (i.e. the duty cycle must be unity). Such a scenario has been shown to be exceedingly unlikely with numerous models and cosmological simulations showing that *light* seeds do not grow efficiently and tend to remain at their seed masses across cosmic time ([Alvarez, Wise & Abel 2009](#); [Milosavljević, Couch & Bromm 2009](#); [Smith et al. 2018](#); [Spinoso et al. 2023](#)).

The reasons for this are complex and multifaceted but are primarily driven by the fact that the *light* seed black holes are unable to sink to, or remain in, the galactic centre where gas densities are higher and also because they must compete for accretion with the star formation processes evolving nearby while local ionising radiation can further hamper accretion. However, in rare circumstances rapid accretion onto a *light* seed may be possible (e.g. Alexander & Natarajan 2014; Zubovas & King 2021; Shi, Kremer & Hopkins 2024). We will return to this topic in §7.

3. HEAVY SEEDS AS A SUB-POPULATION

The need for *heavy* seed black holes has largely been driven by observations of MBHs with masses up to and in excess of $10^9 M_\odot$ at redshifts beyond seven (e.g. Fan, Bañados & Simcoe 2023). With continued observations putting tight constraints on the *light* seed pathway the strong possibility of *heavy* seeds being the progenitors for the MBH which inhabit galactic centres strengthens (e.g. Bogdán et al. 2023; Natarajan et al. 2024).

A number of different avenues remain open to achieving *heavy* seed black holes, including dynamical runaway processes, the direct collapse of a SMS into a MBH and the direct formation of a MBH via galactic mergers. We now briefly discuss the environmental conditions required to drive each of these pathways but refer the interested reader to a review on the subject for a more in-depth analysis (e.g. Inayoshi, Visbal & Haiman 2020; Volonteri, Habouzit & Colpi 2021).

Seminal work by Portegies Zwart et al. (2004) showed that MBHs can be formed through runaway collisions of stars in dense young star clusters. This work has been built on by several groups in more recent years with at times contrasting results (Devecchi & Volonteri 2009; Katz, Sijacki & Haehnelt 2015; Rizzuto et al. 2021; González et al. 2021). The differences can often be ascribed to different initial conditions and environmental factors. For example Arca Sedda et al. (2023) has shown using detailed numerical models using the Nbody6+ +GPU code that in clusters of up to 10^6 stars that black hole growth via stellar collisions tops out at a few hundred M_\odot . While on the other hand simulations by Reinoso et al. (2023) in smaller clusters using the AMUSE (Portegies Zwart et al. 2009; Pelupessy et al. 2013) framework have demonstrated that stellar collisions can grow stars up to several tens of thousands of solar masses when accounting also for gas accretion. In any case, while convergence of results has perhaps not yet been achieved it does appear that initial black hole seed growth up to masses greater than $1000 M_\odot$ does appear viable and hence this route to *heavy* seeds appears plausible (although sensitive to cluster initial conditions). Another related pathway is hierarchical BH mergers within a star cluster undergoing core collapse. In this case repeated black hole mergers can in principle grow a black hole up to masses in excess of $1000 M_\odot$ (Fragione & Leigh 2018; Fragione et al. 2022; Antonini, Gieles & Gualandris 2019; Mapelli et al. 2021; Arca Sedda, Amaro Seoane & Chen 2021). As before however, the final black hole mass is sensitive to the conditions found in the cluster. Nonetheless, again a pathway to *heavy* seed MBH does exist.

In addition to the dynamical pathway *heavy* seeds can form via the formation of a very massive or super-massive star (SMS). In contrast to the formation of a dense cluster and subsequent dynamical runaway inside the cluster a (near-) monolithic collapse is allowed to develop. In this case where fragmentation is suppressed, either through low metallicity or the lack of other efficient coolants, then the possibility of forming very massive or SMSs arises. SMSs are defined by their extremely high accretion rate onto the stellar surface ($\dot{M} \gtrsim 0.001 M_\odot/\text{yr}^{-1}$) which, through the accretion of high entropy gas, causes the photosphere of the star to expand (so long as the accretion rate is maintained, Haemmerlé et al. 2018). Such stars are expected to be very red, in contrast to massive PopIII stars whose spectrum would be blue, and cool with effective temperatures of approximately $T_{\text{eff}} \sim 5000$ K (Hosokawa, Omukai & Yorke 2013; Hosokawa et al. 2013; Haemmerlé et al. 2018; Woods et al. 2021). With maximum theoretical masses of greater than $10^5 M_\odot$ (Woods et al. 2017) these SMS stars would be ideal progenitors for MBHs and among the heaviest seeds possible.

Finally, Mayer et al. (2010, 2015, 2024) have postulated a "direct" mechanism for forming extremely massive black holes. In their model the merger of massive galaxies ($M_{\text{Gal}} \gtrsim 10^{11} M_\odot$) can result in the direct creation of a supermassive black hole with a mass up to $10^8 M_\odot$. The formation of the MBH directly bypasses both the stellar and seed formation stages and may explain the existence of the quasar population seen at $z \sim 6$. However, it cannot explain the existence of less massive black holes at high redshift as the mechanism relies on the merger of massive haloes ($M_{\text{Halo}} \sim 10^{12} M_\odot$ at $z \sim 10$ corresponding to 4σ - 5σ peaks) to drive large gas inflows creating the central MBH.

We note here that high resolution modelling including state-of-the-art physical models is crucial here. When attempting to model the collapse of gas creating the central MBH, resolution and/or physical models can result in fragmenting objects which are unrealistically massive. Early simulations of PopIII formation in particular suffered from this issue (e.g. Bromm, Coppi & Larson 1999; Abel, Bryan & Norman 2000) while more recent approaches (when modelling heavy seed formation) have shown, for example, the importance of resolving dynamical heating (e.g. Wise et al. 2019) and ISM turbulence (e.g. Latif et al. 2022).

4. SEED NUMBER DENSITIES

A crucial question is what are the expected number densities of both *light* and *heavy* seeds in the high- z Universe. *Light* seeds will be ubiquitous in the early universe - forming from the end points of massive stars. The exact number density of *light* seeds is non-trivial to compute and will depend on the initial mass function of the first stars (which is unknown). However, a reasonable estimate would be between $10^{-1} \text{ cMpc}^{-3}$ and up to 10 cMpc^{-3} (at $z \sim 10$) (Xu, Wise & Norman 2013; Smith et al. 2018; Piana et al. 2020; Trinca et al. 2022). The number density of *heavy* seeds will of course be significantly less.

By definition certain, perhaps rare, environmental conditions must occur for heavy seed formation pathways to

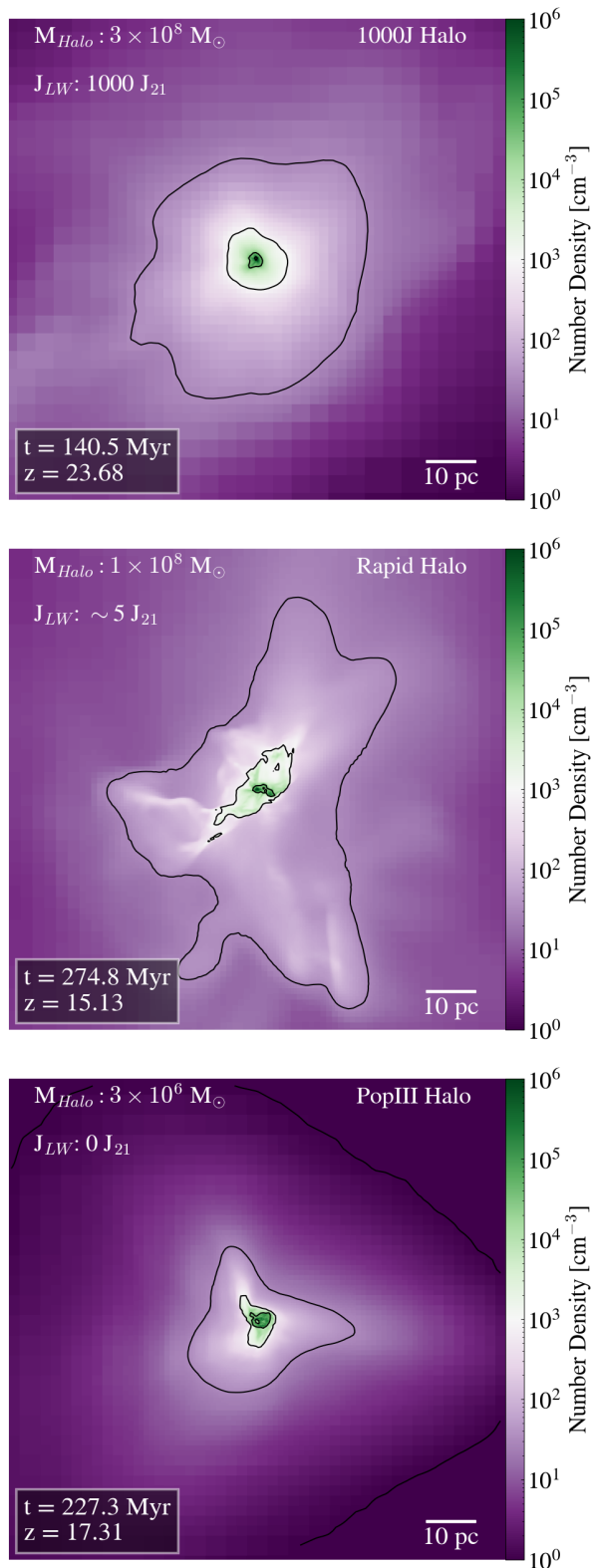


FIG. 2.— Gas Number Density projection plots from each of the three halos selected for our study. In the top panel we show the projection from the 1000J halo, in the middle panel the projection from the Rapid halo and in the bottom panel the PopIII halo. Contours in each panel demarcate density levels in logspace. The 1000J halo (top panel) shows a very symmetric density profile, while both the Rapid (in particular) and PopIII haloes show much more diverse structure. Labelled in each panel is the halo mass, the LW flux impacting onto the halo, the redshift and time of the collapse.

be activated. On the contrary were such conditions common place, we would likely see them in action in the present day universe (at least for cases where gas/stellar metallicity does not need to be very small). Additionally, the rarity and perhaps uniqueness of this pathway to the early Universe has a significant impact on the expected number densities of *heavy* seeds. See Woods et al. (2017); Inayoshi, Visbal & Haiman (2020) for a review of *heavy* seed formation environments.

Dijkstra, Ferrara & Mesinger (2014) calculated the number density of heavy seeds forming through the so-called Lyman-Werner (LW) channel. In this case an atomic halo is irradiated with a super-critical LW by a nearby galaxy (Dijkstra et al. 2008; Agarwal et al. 2012, 2013; Visbal, Haiman & Bryan 2014; Agarwal et al. 2016; Regan et al. 2017). In principle this can lead to the formation of an extremely massive seed (see §5). However, the calculated number densities are small with expected number densities in the range 10^{-10} cMpc^{-3} to 10^{-5} cMpc^{-3} (at $z \sim 10$). It should be noted here that the higher number densities quoted here (i.e. 10^{-5} cMpc^{-3}) should be treated as strong upper limits as they rely on very optimistic formation criteria, namely, low values of the LW radiation needed to keep H_2 dissociated or allowing for metal pollution. Other authors have drawn similar conclusions on the expected number densities from this channel (Inayoshi & Tanaka 2015; Habouzit et al. 2016; Agarwal et al. 2016; Trinca et al. 2022).

Moving now to channels which potentially produce heavy seeds below the theoretical maximum mass (of SMSs) but well in excess of *light* seeds masses. The so-called rapid assembly channel (Yoshida et al. 2003; Fernandez et al. 2014; Wise et al. 2019; Regan et al. 2020c; Lupi, Haiman & Volonteri 2021; Latif et al. 2022) can produce *heavy* seeds with number densities in the range 10^{-5} to 10^{-1} cMpc^{-3} (at $z \sim 10$) (McCaffrey et al. in prep) depending on environmental factors. Number densities achieved through other channels like baryonic streaming velocities result in number densities close to approximately 10^{-5} cMpc^{-3} (at $z \sim 10$) as well (Hirano et al. 2017).

Overall the number densities of *heavy* seeds range over several orders of magnitude (varying according to the expected mass of the seed and the environmental conditions required) from 10^{-10} cMpc^{-3} up to 10^{-1} cMpc^{-3} (at $z \sim 10$). The variance of these estimates spanning almost 10 orders of magnitude speaks to the complexity of the problem. However, what should be kept in mind here is that while producing the heaviest seeds may be exceedingly rare - producing more moderate mass seeds becomes progressively more straightforward and the higher number densities. This leads to the conclusion that even in the case of a *heavy* seed channel that the seed mass function could well be a continuum with a peak at some characteristic mass. We now move on to discuss the types of haloes expected to form both *light* and *heavy* seeds.

5. MODEL HALOES

To illustrate the different environmental conditions that have been investigated in the literature over the last decade or more we have selected three haloes that broadly reflect the mainstream pathways of investigation. Additionally, the environmental conditions required feed directly into the expected number densities

Model Name	Halo Mass [M_{\odot}]	Redshift	Mass of Most Massive Star [M_{\odot}]	Halo Number Density [cMpc^{-3}] at $z \sim 10$
1000J Halo	2.59×10^7	23.70	76123	$10^{-10} - 10^{-5}$
Rapid Halo	9.3×10^7	15.05	6127	$10^{-5} - 10^{-1}$
PopIII Halo	3.7×10^6	17.21	173	$10^{-1} - 10^{+1}$

TABLE 1

CHARACTERISTIC OF THE THREE DIFFERENT HALOES USED TO ILLUSTRATE OUR ARGUMENTS. THE THREE HALOES ARE THE 1000J HALO, THE RAPID HALO AND THE POPIII HALO. FOR EACH HALO WE GIVE THE HALO MASS (SECOND COLUMN), THE REDSHIFT AT WHICH STAR FORMATION FIRST OCCURS IN EACH HALO (THIRD COLUMN), THE MASS OF THE MOST MASSIVE STAR IN EACH HALO (FOURTH COLUMN) AND IN THE LAST COLUMN THE EXPECTED NUMBER DENSITY OF EACH HALO TYPE.

of these seeds. We are not aiming for complete sampling of all scenarios and environments investigated but rather the small sample of haloes selected here reflects in broad terms the emergence of *light* and *heavy* seed pathways. The haloes we select we name the **Rapid** halo, the 1000J halo and the **PopIII** halo. The characteristics of each halo are given in Table 1.

The 1000J halo is the prototypical halo used to test the intense LW field model (see §3 for details). The **Rapid** halo is the result of the rapid assembly paradigm and results in the formation of *heavy* seed black holes via the rapid assembly (or dynamical heating) mechanism. Finally, the **PopIII** halo is a standard mini-halo whose environment is not influenced by either (extreme) LW radiation or rapid assembly. The **PopIII** halo gives rise to *light* seeds while the 1000J halo and **Rapid** halo give rise to *heavy* seeds albeit almost certainly of different initial masses. The expected number densities of seeds as well as their potential mass ranges are given in Table 1. We now discuss each of the haloes in detail comparing and contrasting the different environmental conditions and the reasons why different halo configurations lead to *light* or *heavy* seed formation and whether they offer the potential for significant future growth.

5.1. The 1000J Halo

The 1000J is taken from [Regan & Downes \(2018\)](#) and consists of a single halo irradiated by a LW background field with flux $1000 J_{21}^1$ (an intensity of $1000 J_{21}$ is generally accepted in the literature as required for substantial H_2 suppression (e.g. [Shang, Bryan & Haiman 2010](#))). The simulation evolves with this background field strength until one halo exceeds the atomic cooling threshold. At this point cooling due to Lyman-alpha line emission dominates the cooling and allows the gas to collapse almost isothermally at approximately 8000 K. The most massive star formed in the halo has a mass of approximately $76,000 M_{\odot}$ and there were only four stars in the halo at the end of the simulations (~ 250 kyr after the formation of the first star). This is the proto-typical isothermal collapse seen by most studies in which collapse in the presence of a large LW field is studied ([Latif et al. 2013](#); [Visbal et al. 2014](#); [Latif et al. 2016](#); [Dunn et al. 2018](#); [Schauer et al. 2021](#)). Even larger LW fields may result in less fragmentation at the scales studied while lower LW fields will likely result in more fragmentation (taking into account halo stochasticity).

In the top panel of Figure 2 we show a gas number density projection centred on the 1000J halo. The halo is highly symmetric indicating a near spherical collapse. The symmetry of the halo is also evidenced by the (density-weighted) temperature projection plot shown in

the top panel of Figure 3. The strong LW field homogenises the temperature field leading to a near isothermal collapse (at $\sim 8000\text{K}$). The homogenisation of the temperature field has a knock on effect on the density - making it more homogeneous as well due to the removal of temperature gradients which can lead to cooling instabilities. This in turn leads to less fragmentation. This is an ideal scenario for creating heavy seeds.

In this specific case most of the stellar mass ends up in two SMSs with four SMSs forming in total. The mass of each of the stars is shown in Figure 4. The accretion rate onto the most massive star in the 1000J halo is shown in the top panel of Figure 5 (green line). The SMS accretes at super-critical rates ([Nandal et al. 2023](#)) for more than 200 kyr before the gas supply becomes restricted. The final mass of each of the stars are shown in Figure 4 (green bars). In Figure 5 we show the mass evolution and accretion rate onto the most massive star in the simulation (green lines). The most massive star achieves a mass of more than $76,000 M_{\odot}$ after approximately 250 kyr. At this point the accretion rate falls off as most of the locally available gas is consumed and the star contracts to the main sequence.

The number density of haloes subjected to a super-critical LW flux cannot be obtained from the simulations discussed above due to their idealistic nature. However, both [Visbal, Haiman & Bryan \(2014\)](#) and [Regan et al. \(2020b\)](#) (using the **Renaissance** simulation suite) computed the abundance of so-called synchronised pairs which can lead to the emergence of haloes similar to the 1000J halo ([Regan et al. 2017](#)). Both authors found the abundance of synchronised haloes to be less than 10^{-2}cMpc^{-3} (at $z \sim 10$). However, this number should be seen as an upper limit. For the "Normal" region of the **Renaissance** simulation suite [Regan et al. \(2020b\)](#) found exactly zero synchronised pairs while finding five, in the clustered, "Rarepeak" region. Taking into account the relative rarity of the Rarepeak region, the number densities obtained should be decreased by a factor of approximately 1000. This leads to number densities of less than 10^{-5}cMpc^{-3} (at $z \sim 10$) for a 1000J like object. An important additional point here is that in-situ LW radiation can potentially ease the thresholds somewhat but remains in delicate balance with other factors like metal-pollution which can suppress heavy seed formation (e.g. [Dunn et al. 2018](#); [Bhowmick et al. 2022b](#); [Chiaki et al. 2023](#)).

5.2. The Rapid Halo

The **Rapid** halo is taken from [Regan et al. \(2020c\)](#) which were themselves zoom-in simulations of the **Renaissance** simulation suite. The halo was originally discovered as part of [Wise et al. \(2019\)](#). In this paradigm,

¹ J_{21} is in units of $10^{-21} \text{erg cm}^{-2} \text{s}^{-1} \text{Hz}^{-1} \text{sr}^{-1}$

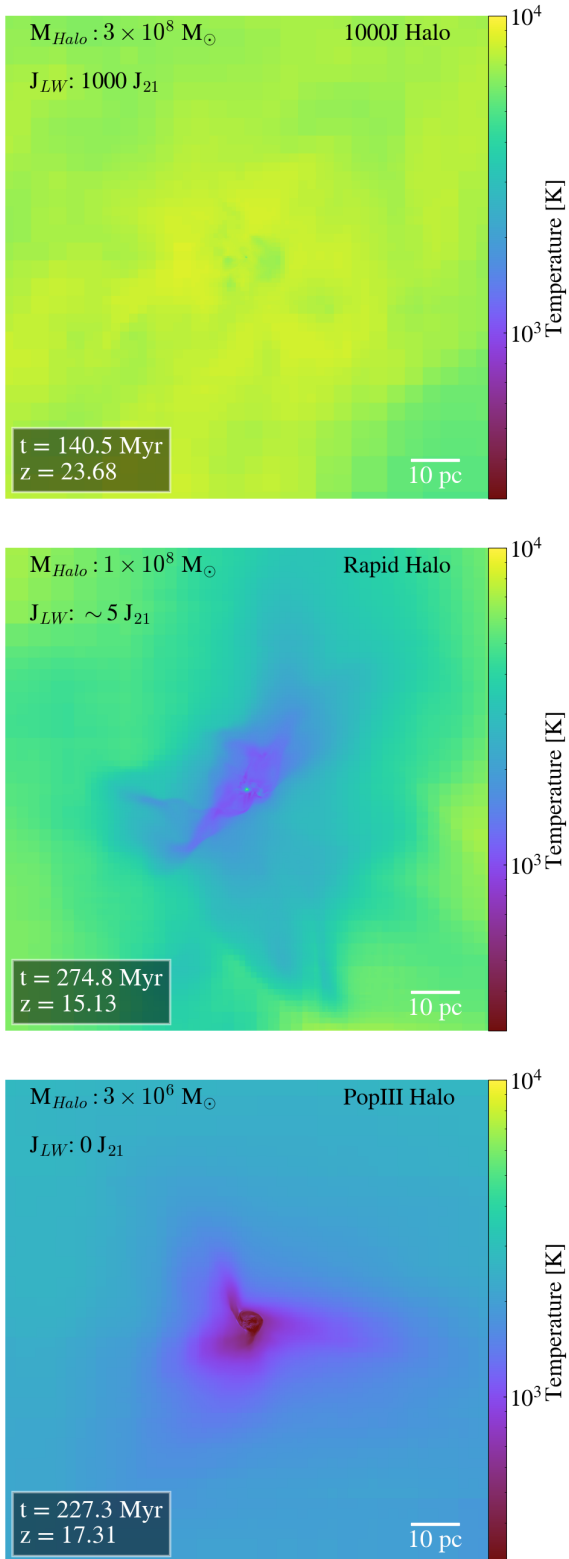


FIG. 3.— Similar to Figure 2 except using the temperature field as the projection variable. In the top panel we show the projection from the 1000J halo, in the middle panel the projection from the Rapid halo and in the bottom panel the PopIII halo. The 1000J shows very little temperature differences reflecting the fact that the strong LW field ($J_{LW} = 1000 J_{21}$) largely dissociates the H_2 ensuring the collapse is isothermal. The middle panel, with only a very mild LW field ($J_{LW} \sim 5 J_{21}$), shows significantly more temperature structure (which drives more structure in the density field). Likewise the bottom panel shows a strong temperature gradient as H_2 is able to cool the gas to below 1000 K in the halo centre.

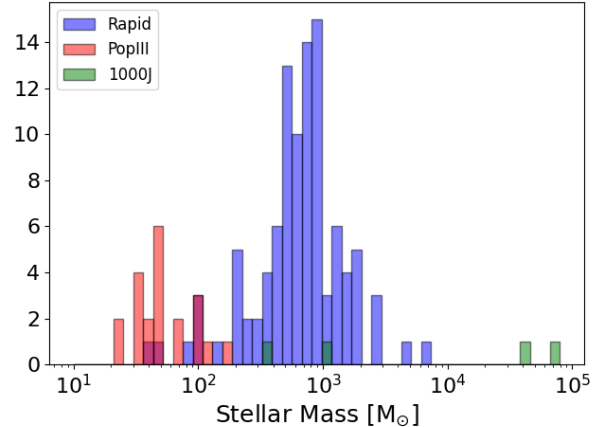


FIG. 4.— The masses of all of the stars formed in each of the three characteristic haloes. Only four stars form in total in the 1000J halo after 250 kyr, approximately 100 in the Rapid halo after 2 Myr while the PopIII halo forms approximately 20 stars after 2 Myr. The masses of the stars formed in the 1000J are up to an order of magnitude more massive than those in the Rapid halo and more than two orders of magnitude more massive than those formed in the PopIII halo.

as described in §3, the halo experiences periods of extremely rapid growth, which dynamically heats the halo, overcoming the ability of H_2 to cool the gas. As a result the gas stays ‘hot’ increasing the Jeans mass of any fragmenting clumps (and reducing the number of fragmenting clumps) - see also [Latif et al. \(2022\)](#) who explore a similar case to that of [Wise et al. \(2019\)](#) albeit in a rarer environment.

The gas number density distribution of the halo is shown in the middle panel of Figure 2. The morphology is clearly very different to that of the 1000J shown in the panel above. In the case of the Rapid halo there is a distinct lack of symmetry. The (density-weighted) temperature projection shows a similar diversity compared to the 1000J halo. The temperature distribution with cooler gas towards the centre clearly contains far more structure. The Rapid halo forms 99 stars over the course of 2 million years with the most massive star having a mass of $6127 M_{\odot}$ at the end of the simulation. The mass of each star at the end of the simulation is shown in Figure 4 (blue bars). The halo has a peak star mass of approximately $1000 M_{\odot}$. The mass of the most massive star and the accretion rate onto the most massive star in the Rapid halo is shown, as a function of time, in Figure 5 (blue lines). Similarly, to the 1000J the most massive star stops accreting after a few tens of kyr as the locally available gas supply runs out. At this point the star contracts to the main sequence and becomes a massive (and extremely luminous) PopIII star.

The number density of rapidly growing haloes from the Renaissance simulations is approximately $5 \times 10^{-3} \text{ cMpc}^{-3}$ at $z \sim 10$ ([Regan et al. 2020a](#))². This is at least two orders of magnitude higher than the probability of forming a 1000J like object. The criteria used to define these haloes from the Renaissance simulations was all haloes with mass inflow rates exceeding $0.1 M_{\odot}/\text{yr}^{-1}$ in the halo centre and with metallicities $Z \lesssim 10^{-3} Z_{\odot}$.

² This value is taken from the ‘Normal’ simulation which runs to $z = 11.6$

5.3. The PopIII Halo

As with the **Rapid** halo the PopIII Halo is taken from [Regan et al. \(2020c\)](#). The halo represents a canonical mini-halo with no LW field flux or rapid assembly. The PopIII halo forms PopIII stars out of primordial Hydrogen and Helium. The bottom panel of Figure 2 shows the gas number density projection of the collapsing PopIII halo. The collapse is somewhat symmetric while also showing clear evidence of an extended morphology. Similarly, the (density-weighted) temperature projection shown in the bottom panel of Figure 3 shows a clear temperature gradient with cooler gas forming deeper inside the halo. The PopIII halo forms 21 stars by the end of the simulation with the most massive star having a mass of $173 M_{\odot}$ (see Figure 4, red lines). The top panel of Figure 5 shows the cumulative mass as a function of time for the most massive star (red line) while the bottom panel shows the accretion rate onto the most massive star in the PopIII halo.

The number density of haloes, at $z \sim 10$, in the Renaissance simulation suite hosting *light* seeds (i.e. PopIII remnant black holes) is approximately 0.3 cMpc^{-3} . This is approximately 10^3 times higher than the number density of rapidly accreting haloes from the same simulation volume and at least 10^5 times higher than the number density of LW haloes expected in a similar volume.

6. MODEL HALO COMPARISON

Differences are clearly apparent across the three characteristic haloes chosen. The 1000J has a near homogeneous density distribution as a result of the super-critical LW flux it is exposed to. This density (and temperature) homogeneity promotes a strong suppression of fragmentation resulting in two extremely massive objects forming (masses of $76000 M_{\odot}$ and $44000 M_{\odot}$) along with two less massive stars. The other two haloes (**Rapid** and **PopIII**) show a more inhomogeneous density (and temperature) distribution (due to the presence of higher H_2 fractions) and result in lower mass stars. The distribution in stellar masses across each halo is shown in Figure 4 with the 1000J showing fewer but significantly more massive stars compared to either the **Rapid** halo or the **PopIII** halo.

There are two primary reasons for the elevated stellar masses found in the 1000J compared to the **Rapid** and **PopIII** halo. On the one hand and as described above the LW flux dissociates H_2 and leads to larger Jeans masses and hence larger protostars ([Prole et al. 2024](#)) but also these protostars can accrete more readily and for longer (see Figure 5). In the **Rapid** halo and **PopIII** halo the structures are far more asymmetric making continued accretion much more difficult (at least for the stellar masses probed here). For the cases of stars in both the **Rapid** and **PopIII** haloes the stars can initially accrete gas readily but the gas supply quickly gets consumed and the stars contract to the main sequence ([Regan et al. 2020c](#)) with masses significantly below that seen in more symmetric and homogeneous halos.

It should be noted that in Figure 5 we show only accretion over a relatively short period (hundreds of kiloyears). The time-resolution needed for these simulations is very short - of the order of years compared to large

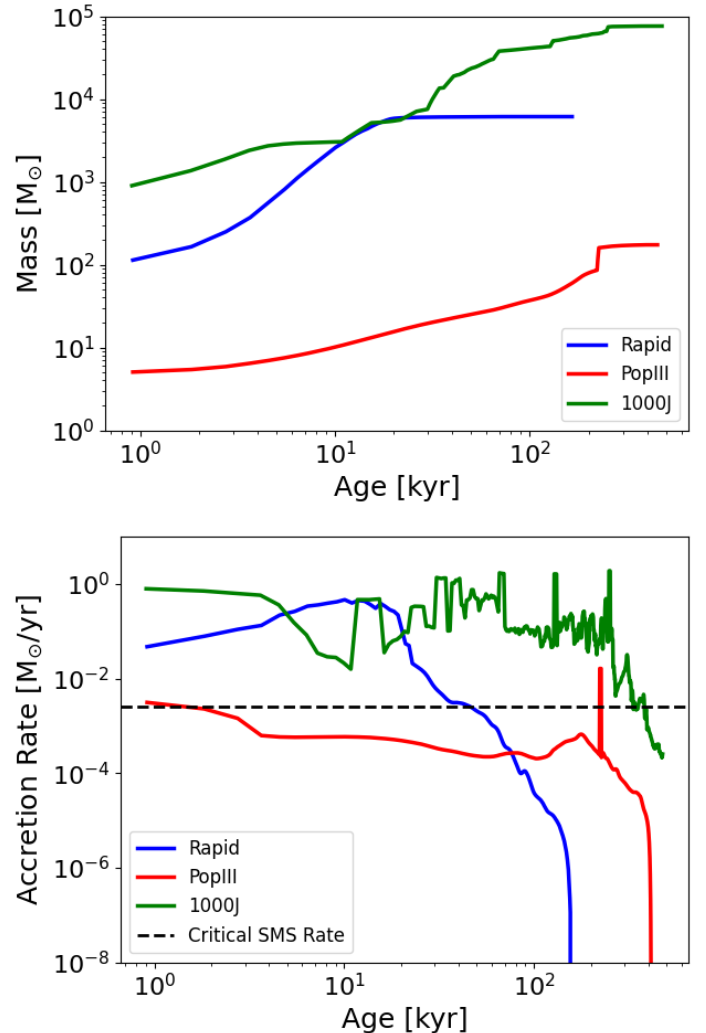


FIG. 5.— The evolution of the most massive star that forms in each of the three haloes (1000J, **Rapid** and **PopIII**). Stars are modelled as accreting sink particles. The spatial resolution of each simulation is approximately 10^{-3} pc (physical). In the top panel we show the mass as a function of time. In the bottom panel we show the accretion rate onto the most massive star in each halo as a function of time. The 1000J halo forms the most massive object followed by the **Rapid** halo and the **PopIII** halo. The dashed line shows the critical accretion that must be maintained onto the stellar surface to meet the criteria for being a super-massive star ([Nandal et al. 2023](#)).

scale cosmological simulations with timesteps many orders of magnitude higher. The subsequent growth of the seed (*light* or *heavy*) will depend fundamentally on the evolution of the host galaxy over several tens and hundreds of megayears. Presently, simulations able to track the model the formation of *light* and *heavy* seeds and to subsequently follow their growth are extremely computationally challenging and essentially intractable. We nonetheless describe progress in this direction in the following section bearing in mind that this remains an extremely challenging modelling problem.

7. BLACK HOLE GROWTH

The sustained growth of black holes is clearly critical for their evolution into the MBHs we observe as both high-

z quasars and as the "JWST-quasars" at $z \gtrsim 7$. The question then becomes which seeds are more likely to experience significant growth?

7.1. Growth of Light Seeds

Light seeds can suffer from initially severely stuttered growth as a result of their formation pathway. Depending on their final mass the seeds are often born "starving" into an environment which is hostile to initial growth (e.g. Whalen, Abel & Norman 2004; Alvarez, Wise & Abel 2009; Milosavljević, Couch & Bromm 2009). This is because the ionising feedback from the stellar phase plus the energy injected into the surrounding gas results in a *light* seed born into a relatively underdense local environment.

Light seeds can nonetheless grow in two ways, firstly via gas accretion and secondly via mergers with other compact objects. Due to their smaller masses *light* seeds have a significantly smaller Bondi radius (which scales as M_{BH}^2) compared to *heavy* seeds. Furthermore, their mass relative to that of their host galaxy and indeed the surrounding stellar and gas distribution is negligible. This means that *light* seed black holes will tend to move easily within their environment - a movement which can appear random. A number of authors have investigated this property of *light* seeds numerically.

Smith et al. (2018) et al. used the *Renaissance* suite to track, in post-processing, the evolution of *light* seed black holes formed from PopIII stars. They tracked the evolution of over 20,000 *light* seeds for up to 200 Myrs and found negligible growth across the entire *light* seed population. The reason being is that the *light* seeds experience extremely low duty cycles due to the surrounding (negative) feedback processes of star formation and stellar feedback. Moreover, higher resolution studies of (PopIII) star forming environments show that PopIII stars form in multiples (e.g. Turk, Abel & O'Shea 2009; Clark et al. 2011; Prole et al. 2024) setting off a competitive accretion scenario further mitigating against efficient accretion. Other authors (e.g. Pfister et al. 2019; Ma et al. 2021) find that only seeds with masses in the *heavy* seed (up to $10^8 M_\odot$ in the case of the Ma et al. (2021) study) range can effectively sink to the centre of the potential well where efficient accretion may be sustainable. None of the above studies rule out *light* seed accretion but instead find that the probability of efficient *light* seed growth is extremely low.

Building on these challenging conclusions from studies of *light* seed growth a number of groups have investigated how growth can be accelerated when the conditions are favourable. In the majority of these cases the *light* seed black hole is modelled to either sit at the centre of a converging flow (e.g. Volonteri & Rees 2005) or is "trapped" within the confines of a nuclear star cluster (Alexander & Natarajan 2014; Natarajan 2020) or within a circumnuclear disk (e.g. Lupi et al. 2016). More recent work by Shi, Kremer & Hopkins (2024) shows that a small fraction ($\sim 1\%$) of *light* seeds can achieve bursts of rapid growth when placed in environments that are favourable (i.e. are gas rich and support growth). In each of these cases the growth of the initially *light* seed proceeds via bursts of super-Eddington accretion. The physical process of super-Eddington accretion has been

demonstrated extensively via extremely high resolution simulations (e.g. Sądowski 2009; Sądowski & Narayan 2016; Sądowski et al. 2016; Jiang, Stone & Davis 2019; Jiang et al. 2020). However, what is lacking are robust numerical simulations which show self-consistently the growth of *light* seeds in a cosmological setting. The reason for this is that a combination of high resolution, with resolved dynamics, and a realisation containing a rare dynamical occurrence is required. This has, thus far, not been realised. However, such a setup should be tractable with current simulation codes and techniques at least for the early evolutionary phase.

In the above discussion we have focused on growth through gas accretion. However, a *light* seed can grow also via mergers. The classic case here is a dense stellar cluster where stars undergo collisions resulting in *light* or *heavy* seed formation and the seed subsequently merges with other stars and BHs resulting in a final seed mass. The final seed mass attainable here is unclear and detailed state-of-the-art n-body simulations have not yet converged on a final result (e.g. Arca Sedda et al. 2023; Rantala, Naab & Lahén 2024) due to the complex parameter space that must be explored. Additionally, the impact of gas on both the dynamics and accretion must be incorporated into this scenario and this could potentially result in much larger seed masses (e.g. Chon & Omukai 2020; Reinoso et al. 2023).

Conversely, *light* seed mergers in the aftermath of galaxy mergers (the classic case considered, for instance, to estimate merger rates for gravitational wave detectors such as LISA) is unlikely. This is because of the same reasons why sinking and retaining *light* seeds in galaxy centres is difficult, as already discussed. In a galaxy merger a *light* seed will have mass not much larger than that of stars and therefore dynamical friction is inefficient: the probability that two *light* seeds, which have very small cross section, find each other within this sea of stars is exceedingly small.

7.2. Heavy Seed Growth

Given that the growth of *light* seeds appears very inefficient in the main, it is worth exploring whether *heavy* seeds can avoid this bottleneck. As discussed above this will likely depend sensitively on the mass of the *heavy* seed. Pfister et al. (2017) showed that growth is extremely inefficient below at least $10^5 M_\odot$ and perhaps as high as an initial mass of $10^8 M_\odot$ in the case of Ma et al. (2021). These seminal works appear to be borne out by more recent simulations. For example Lupi et al. (2024) model the progenitor of a high-z quasar using an initial black hole seed mass of $10^5 M_\odot$ (the model sets the initial dynamical mass of the *heavy* seed to be $10^6 M_\odot$). This initial mass helps to stabilise the seed prior to rapid growth - nonetheless the initial growth is stunted by supernova feedback and requires significant halo growth to facilitate the black hole growth (see also Bhowmick et al. 2022a). Although the initial barrier to growth depends on the strength of supernova feedback, what this shows is that growth can occur onto a *heavy* seed but only if the seed is massive and if the conditions are favourable (i.e. the halo is sufficiently massive). Latif & Khochfar (2020) reached similar conclusions, albeit from somewhat

more idealised conditions - following the growth of a *heavy* seed ($M_{\text{seed}} = 10^5 M_{\odot}$) starting from a halo similar to the 1000J halo described above.

On larger scales the Astrid (e.g. Bird et al. 2022; Ni et al. 2022), NewHorizon (Dubois et al. 2021; Beckmann et al. 2022) and Romulus (e.g. Tremmel et al. 2017; Ricarte et al. 2019) simulation suites all seed black holes with masses well inside the *heavy* seed regime as well as implementing dynamical friction subgrid modelling. For higher mass galaxies the results for the simulation suites are broadly consistent. However, for smaller mass galaxies ($M_* \lesssim 10^9 M_{\odot}$), the results are not converged. Ricarte et al. (2019) show that MBHs can grow in galaxies independent of the stellar mass (and hence show little or no effect from supernova feedback). This is in contrast to other results (e.g. Dubois et al. 2014; Habouzit, Volonteri & Dubois 2017; Anglés-Alcázar et al. 2017). The reasons for this difference are not obvious and require further investigation (Ricarte et al. 2019).

So overall where does the extensive work on black hole growth leave us? Across the various simulation setups there is convergence that black holes can grow once the host halo becomes massive enough with some differences arising for black hole growth in lower mass galaxies which needs to be fully understood. Additionally, the black hole must achieve a mass of at least $10^5 M_{\odot}$ before growth can be achieved - this is particularly evident from the Astrid simulations which have the lowest seed masses ($M_{\text{seed}} \gtrsim 10^4 M_{\odot}$) and see very limited growth for the lightest seeds. Similar results are obtained in semi-analytical models (Trinca et al. 2022; Spinoso et al. 2023). The main result therefore is that any MBH seeds below approximately $10^5 M_{\odot}$ grow extremely inefficiently due to dynamics. In addition to this, in low mass galaxies ($M_* \lesssim 10^9 M_{\odot}$) growth may be hampered by supernova feedback but this result suffers from different interpretations in the literature and requires further study.

8. SUMMARY AND CONCLUSIONS

The goal of this paper is to weave together recent developments in modeling MBH seeding and pathways to their growth. The current paradigm is broken into *light* and *heavy* seeds with *light* seeds typically defined as those with initial masses less than $1000 M_{\odot}$ and *heavy* seeds as those with initial masses in excess of $1000 M_{\odot}$ (e.g. Sasano et al. 2021; Evans, Blecha & Bhowmick 2023; Jeon et al. 2024). Scenarios considered in the past gave rise to a bimodal initial mass function: common *light* seeds related to PopIII stars with mass $\sim 100 M_{\odot}$ and rarer *heavy* seeds related to SMSs with mass $\sim 10^5 M_{\odot}$. In order to grow these seeds into the massive and super-massive regime, two main pathways were considered: super-Eddington on *light* seeds and sub-Eddington on *heavy* seeds, although of course super-Eddington accretion can occur, and indeed it may be more likely to occur, for *heavy* seeds. What the most recent simulations are instead suggesting is that these two regimes are likely to be the extreme cases of a broad distribution of initial properties.

To characterise the pathways to achieving each seed (*light* or *heavy*) we select three representative haloes

which we use to illustrate the different environmental conditions in which they form. Our findings regarding seed *formation* are as follows:

1. **The heaviest seeds:** Haloes subjected to a strong or super-critical LW flux will most likely result in the largest single stellar object forming, up to $\sim 10^5 M_{\odot}$ (1000J halo). This is because the absence of any coolant, apart from Hydrogen, results in a halo whose temperature is nearly uniform across the halo inducing a near spherical collapse. Such conditions are very rare (seed number densities $\sim 10^{-10} - 10^{-5} \text{ cMpc}^{-3}$ at $z \sim 10$) and cannot explain the number densities of either the high- z AGN population or the local MBH population.
2. **Heavy seeds:** Other mechanisms that lead to environments conducive to heavy seed formation (e.g. a rapid assembly process, baryonic streaming velocities or mechanisms that lead to the emergence of dense stellar systems) but not necessarily a monolithic collapse will generate a spectrum of heavy seed masses. In this, more fragmented, environment heavy seed multiplicity will be higher with the mass therefore spread across more fragments. For the specific examples shown here the largest stellar masses are up to $\sim 10^4 M_{\odot}$ (e.g. in the Rapid halo). However, the number densities are up to $\sim 10^5$ times higher than in the monolithic case making it possible to explain the number density of the whole massive BH population.
3. **Light Seeds:** Smaller haloes or those enriched with metals will produce relatively less massive stars. These stars will be distributed inhomogeneously around the halo centre and will accrete very inefficiently. The largest stellar masses shown here have masses up to a few times $\sim 10^2 M_{\odot}$ (PopIII halo). The number densities of these halos are between $10^{-1} \text{ cMpc}^{-3}$ and up to 10 cMpc^{-3} ($z \sim 10$).

Based on these findings and results of other investigations, we speculate on seed *growth* as follows:

1. **Need for gas replenishment:** In all three halos considered the accretion rate on the stellar progenitors of the seeds drops after $\sim 10^5$ years as the readily accretable gas in the parent halo is consumed. Gas replenishment is needed (Johnson & Bromm 2007; Lupi et al. 2024) through either mergers with gas-rich halos or accretion from the cosmic web.
2. **Light Seed Accretion:** *Light* seeds accrete inefficiently because of a combination of a small Bondi radius (Pacucci et al. 2017) and their collective dynamics that leads them to move randomly in the inhomogenous stellar+dark matter distribution (Smith et al. 2018; Pfister et al. 2019). In order to overcome this barrier, some mechanism is necessary to allow highly efficient and sustained accretion to take place: for instance if they are embedded in a star cluster (Alexander & Natarajan 2014; Natarajan 2020), are captured/capture gas clumps (Lupi et al. 2016) or a later merger brings them into an

extremely gas rich region (Johnson & Bromm 2007; Pezzulli, Valiante & Schneider 2016). The question is for how long the BHs are able to remain within this dense region?

3. **Heavy Seed Accretion:** *Heavy* seeds experience the same bottlenecks as *light* seeds, but their effect is mitigated in relation to the seed masses: Bondi accretion scales as M_{BH}^2 and gravity scales as M_{BH} . A 10-times more massive seed has better chances of remaining in dense regions and accreting from them (Pfister et al. 2019; Lupi et al. 2024).
4. **Light Seed Mergers:** The more erratic dynamics and small cross-section of *light* seeds will hamper their growth by BH-BH mergers except when they are located in dense stellar environments (Reinoso et al. 2023; Arca Sedda et al. 2023; Rantala, Naab & Lahén 2024). After a galaxy merger existing seeds with masses below $\sim 10^5 M_{\odot}$ are highly unlikely to bind in binaries (Pfister et al. 2019; Ma et al. 2021).
5. **Heavy Seed Mergers:** similarly to what was described for accretion, *heavy* seeds are favored proportionally to their mass, since gravity-related process are eased as the BH mass increases, but even *heavy* seeds have a hard time reaching the “center” of the shallow and granular potential of high-redshift galaxies (Ma et al. 2021).

In summary *heavy* seeds production is more likely the more symmetric the halo is. The advance of more sophisticated models and simulations over the last two decades in particular tracks this idea well. Initially the relatively coarse simulations which also lacked advanced cooling algorithms showed the formation of central massive stars (e.g. Abel, Bryan & Norman 2000; Bromm, Coppi & Larson 1999). The inclusion of more sophisticated simulations at increased resolution has in the vast majority of cases led to more fragmentation and a more complex morphology within collapsing haloes, for both *light* and *heavy* seed scenarios.

While *heavy* seed formation has still been shown to be viable in these more sophisticated simulations the most massive objects formed tend to be lighter than the maximum mass (theoretically) possible. Moreover, while *light* seeds will be abundant with characteristic masses in the range of a few tens of solar masses they will be scattered around a morphologically complex halo. Rapid growth in such an environment will be extremely unlikely. Indeed the growth of *heavy* seeds in such an environment is still challenging albeit mitigated by the larger Bondi radius which scales as M_{BH}^2 .

So then the question becomes - what seeds will grow and within what environment? Rapid growth will only become viable if a seed (light or heavy) can sink towards and remain in the galaxy centre where the gas densities are highest. The heavier the initial mass the more likely this is to occur. *Light* seeds, in isolation, are not likely to do this, but there are regions of the parameter space that allow for their growth. Smith et al. (2018) showed in their study that out of 20,000 *light* seeds none grew: this suggests that the fraction of *light* seeds able to grow is less than 10^{-4} . More

optimistically Shi, Kremer & Hopkins (2024) find that the fraction of light seeds that grow, under favourable and somewhat idealised assumptions, is $\sim 10^{-2}$. If the *light* seed that grows is able to reach the typical mass of a *heavy* seed, and the abundance of *light* seeds is at least $10^3 - 10^4$ times that of *heavy* seeds then *light* seeds become equally likely to be the source of MBHs. A point of note here is that it is currently impossible to constrain seed models based on current observational data of MBH masses by extrapolating the growth backwards. The available parameter space, which allows both Eddington and super-Eddington phases makes this an impossible challenge. All that can be garnered from current observational data is an upper limit on the seed masses.

9. OUTLOOK

The most recent generation of large scale hydrodynamical simulations are beginning to achieve mass and spatial resolutions at a level where self-consistently tracking light and heavy seed formation and growth becomes tractable. As discussed in §7 the Astrid, NewHorizon and Romulus simulation suites already model *heavy* seed-like objects and study their growth over cosmic timescales. While the formation of the heavy seeds from either a stellar or collisionally driven pathway is not followed self-consistently the subsequent growth through accretion and mergers of the MBH is followed reasonably accurately. Moreover, the simulations include subgrid models for dynamical friction which model the dynamics of these *heavy* seed black holes within growing proto-galaxies.

Semi Analytic Models (SAMs) rely on a backbone of dark matter merger trees to model galaxy and MBH evolution over long timescales. Their relative simplicity, compared to hydrodynamic simulations make them ideal for rapidly traversing the large parameter space of galaxy and black hole formation (e.g. Schneider et al. 2006; Dayal et al. 2019; Trinca et al. 2022). However, this power comes at the cost of small scale details. SAMs inherently do not have spatially-resolved structures and the detailed physical modelling capacity necessary to capture emergent physics like turbulence, detailed ISM physics as well as the likely episodic nature of MBH accretion.

In Figure 6 we show a schematic outlining the range of spatial and temporal scales that must be bridged by our models. No one simulation suite, technique or code can cross the domains and multiple suites and techniques (SAMs + hydrodynamics) must be used. To model MBH evolution different models utilise different seeding and accretion prescriptions - usually driven by the numerical resources available to them at a given scale. For example the large scale simulations (top right) must seed galaxies with relatively large black holes which represent black holes not necessarily at their seed masses but at some time after their physical formation.

SAMs based on high-resolution parent DM halo trees can in principle seed MBHs in arbitrarily low-mass galaxies/halos. However, SAMs have to seed BHs based on global quantities rather than local, spatially-resolved properties. Common to both the large scale hydrodynamic simulations and the SAMs is a difficulty in resolving the dynamics and detailed accretion physics of the MBHs. As we negotiate the parameter space of the

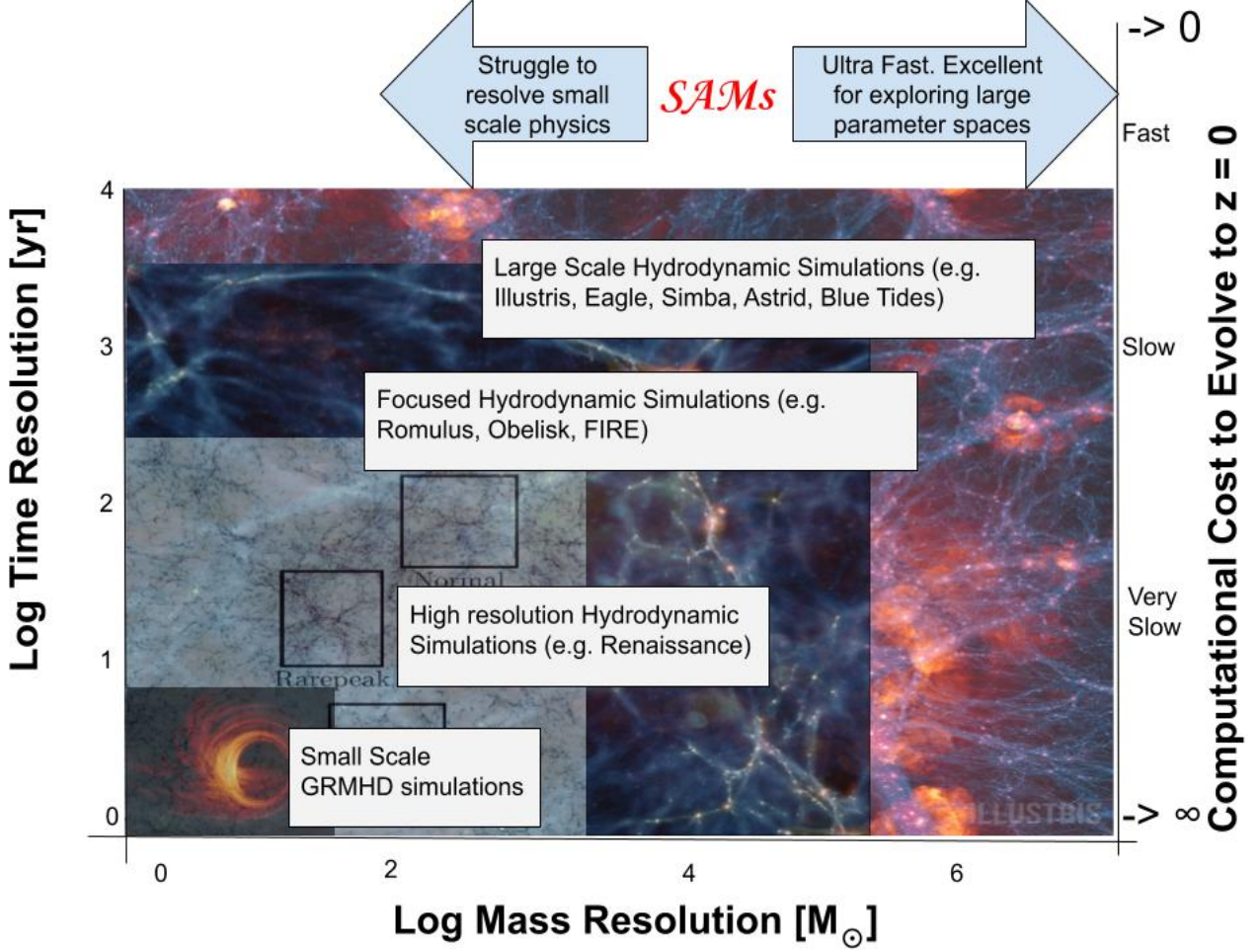


FIG. 6.— Schematic comparing Semi Analytic Models (SAMs) against hydrodynamic simulations. The computational complexity increases from the top right to the bottom left. Models in the top right run extremely quickly but can lack the physical complexity to resolve small scale features like MBH dynamics and seed formation. On the other hand models occupying the bottom left panel focus on scales close to the event horizon and can only be evolved for relatively short physical times given the extreme computational expenses. An array of simulations volumes and resolutions must therefore be used to "join" the scales. The simulation images shown include Illustris (e.g. Vogelsberger et al. 2014), Romulus (e.g. Tremmel et al. 2017), Renaissance (e.g. Xu, Wise & Norman 2013) and results from small scale GRMHD simulations (Chatterjee et al. 2019).

schematic moving from top right to bottom left the models can become increasingly sophisticated in how, and at what mass, black holes are seeded. At smaller scales and higher resolution emergent physics gives rise to a better handle on the physics thought necessary for MBH formation (be they light or heavy seeds). Conversely, these simulations are unable, to follow over long timescale, the evolution of the seeds.

The next generation of simulations are likely to push this mass resolution limit even further slowing encroaching into the regime of the *light* seed (simulations by Bhowmick et al. (2024a,b) already incorporate some of this thinking, albeit with optimistic dynamics as BHs are pinned to halo centres, increasing the chances of growth by both accretion and mergers). By including a self-consistent treatment of both *light* and *heavy* seeds and their dynamics, the growth and relative number densities of each seed population can in principle be determined. However, expectations must be tempered. For the foreseeable future a subgrid model for both *light* and *heavy* seed formation will exist particularly as the formation pathways for *heavy* seeds via collisional runaway

(e.g. Arca Sedda et al. 2023; Rantala, Naab & Lahén 2024) and via SMSs remain unconverged in detailed high resolution simulations (e.g. Prole et al. 2024).

From the observational point of view, JWST has detected a new population of AGN, selected spectroscopically via broad (Maiolino et al. 2024b; Matthee et al. 2024) or narrow emission lines (Scholtz et al. 2023), or photometrically via color-color selection and then followed up spectroscopically to identify broad emission lines (Greene et al. 2024). This population has a number density above the extrapolation of the previously-known bright end of the AGN luminosity function: this is because these AGN have little or no X-ray emission (Furtak et al. 2024; Yue et al. 2024b) and they are UV-faint with respect to the host galaxies (Matthee et al. 2024; Scholtz et al. 2023). The physical reason for this is still unclear, but previous selections were based on X-ray and restframe-UV, and therefore this population was missed. Interestingly, reanalysis of HST images using variability has uncovered a similarly sized population that is UV bright (Hayes et al. 2024) and some of the high-*z* AGN are X-ray bright (Bogdán et al. 2023). However, as a

population, the JWST AGN, or perhaps candidates, do not show X-ray emission (Yue et al. 2024a; Maiolino et al. 2024a; Ananna et al. 2024). This lack of X-rays has led to different hypotheses: the sources are not AGN, they're AGN but the masses of MBHs have been overestimated, or they are intrinsically X-ray weak, or they are surrounded by dust-free Compton-thick gas.

These sometimes conflicting results make it difficult to anchor theoretical models to observations, and in these early days of these new JWST results we may consider taking an agnostic attitude and perhaps consider the AGN as candidates, while waiting for additional in-depth analyses. No doubt, however, this influx of data to previously inaccessible wavelengths has opened new pathways to test and constrain theoretical models of MBH formation and growth by accretion. In the not

too far future, LISA and ET will probe MBH growth by mergers for massive and intermediate-mass BHs up to very high redshift (eLISA Consortium et al. 2013; Maggione et al. 2020).

ACKNOWLEDGEMENTS

We thank the referee for providing highly constructive feedback which greatly improved the manuscript. JR acknowledges support from the Royal Society and Science Foundation Ireland under grant number URF\R1\191132. JR also acknowledges support from the Irish Research Council Laureate programme under grant number IRCLA/2022/1165. MV acknowledges funding from the French National Research Agency (grant ANR-21-CE31-0026, project MBH_waves).

REFERENCES

- Abel T., Bryan G. L., Norman M. L., 2000, *ApJ*, 540, 39
- Agarwal B., Davis A. J., Khochfar S., Natarajan P., Dunlop J. S., 2013, *MNRAS*, 432, 3438
- Agarwal B., Khochfar S., Johnson J. L., Neistein E., Dalla Vecchia C., Livio M., 2012, *MNRAS*, 425, 2854
- Agarwal B., Smith B., Glover S., Natarajan P., Khochfar S., 2016, *MNRAS*, 459, 4209
- Alexander T., Natarajan P., 2014, *Science*, 345, 1330
- Alonso-Álvarez G., Cline J. M., Dewar C., 2024, arXiv e-prints, arXiv:2401.14450
- Alvarez M. A., Wise J. H., Abel T., 2009, *ApJ*, 701, L133
- Ananna T. T., Bogdán Á., Kovács O. E., Natarajan P., Hickox R. C., 2024, *ApJ*, 969, L18
- Anglés-Alcázar D., Faucher-Giguère C.-A., Quataert E., Hopkins P. F., Feldmann R., Torrey P., Wetzel A., Kereš D., 2017, *MNRAS*, 472, L109
- Antonini F., Gieles M., Gualandris A., 2019, *MNRAS*, 486, 5008
- Arca Sedda M., Amaro Seoane P., Chen X., 2021, *A&A*, 652, A54
- Arca Sedda M., Kamlah A. W. H., Spurzem R., Rizzuto F. P., Naab T., Giersz M., Berczik P., 2023, *MNRAS*, 526, 429
- Bañados E. et al., 2018, *Nature*, 553, 473
- Beckmann R. S. et al., 2022, arXiv e-prints, arXiv:2211.13301
- Bhowmick A. K. et al., 2022a, *MNRAS*, 516, 138
- Bhowmick A. K., Blecha L., Torrey P., Kelley L. Z., Vogelsberger M., Nelson D., Weinberger R., Hernquist L., 2022b, *MNRAS*, 510, 177
- Bhowmick A. K., Blecha L., Torrey P., Weinberger R., Kelley L. Z., Vogelsberger M., Hernquist L., Somerville R. S., 2024a, *MNRAS*, 529, 3768
- Bhowmick A. K., Blecha L., Torrey P., Weinberger R., Kelley L. Z., Vogelsberger M., Hernquist L., Somerville R. S., 2024b, *MNRAS*, 529, 3768
- Bird S., Ni Y., Di Matteo T., Croft R., Feng Y., Chen N., 2022, *MNRAS*, 512, 3703
- Bogdán Á. et al., 2023, *Nature Astronomy*
- Boylan-Kolchin M., 2023, *Nature Astronomy*, 7, 731
- Bromm V., Coppi P. S., Larson R. B., 1999, *ApJ*, 527, L5
- Carr B., Silk J., 2018, *MNRAS*, 478, 3756
- Chatterjee K., Liska M., Tchekhovskoy A., Markoff S. B., 2019, *MNRAS*, 490, 2200
- Chiaki G., Chon S., Omukai K., Trinca A., Schneider R., Valiante R., 2023, *MNRAS*, 521, 2845
- Chon S., Omukai K., 2020, *MNRAS*
- Clark P. C., Glover S. C. O., Smith R. J., Greif T. H., Klessen R. S., Bromm V., 2011, *Science*, 331, 1040
- Dayal P., Rossi E. M., Shiralilou B., Piana O., Choudhury T. R., Volonteri M., 2019, *MNRAS*, 486, 2336
- Devecchi B., Volonteri M., 2009, *ApJ*, 694, 302
- Dijkstra M., Ferrara A., Mesinger A., 2014, *MNRAS*, 442, 2036
- Dijkstra M., Haiman Z., Mesinger A., Wyithe J. S. B., 2008, *MNRAS*, 391, 1961
- Dubois Y. et al., 2021, *A&A*, 651, A109
- Dubois Y. et al., 2014, *MNRAS*, 444, 1453
- Dunn G., Bellovary J., Holley-Bockelmann K., Christensen C., Quinn T., 2018, *ApJ*, 861, 39
- eLISA Consortium et al., 2013, ArXiv e-prints 1305.5720
- Evans A. E., Blecha L., Bhowmick A. K., 2023, arXiv e-prints, arXiv:2309.11324
- Fan X., Bañados E., Simcoe R. A., 2023, *ARA&A*, 61, 373
- Fan X., Carilli C. L., Keating B., 2006, *ARA&A*, 44, 415
- Feng W.-X., Yu H.-B., Zhong Y.-M., 2021, *ApJ*, 914, L26
- Fernandez R., Bryan G. L., Haiman Z., Li M., 2014, *MNRAS*, 439, 3798
- Fragione G., Kocsis B., Rasio F. A., Silk J., 2022, *ApJ*, 927, 231
- Fragione G., Leigh N., 2018, *Monthly Notices of the Royal Astronomical Society*, 480, 5160
- Furtak L. J. et al., 2024, *Nature*, 628, 57
- González E., Kremer K., Chatterjee S., Fragione G., Rodriguez C. L., Weatherford N. C., Ye C. S., Rasio F. A., 2021, *ApJ*, 908, L29
- Greene J. E. et al., 2024, *ApJ*, 964, 39
- Habouzit M., Volonteri M., Dubois Y., 2017, *MNRAS*, 468, 3935
- Habouzit M., Volonteri M., Latif M., Dubois Y., Peirani S., 2016, *MNRAS*, 463, 529
- Haemmerlé L., Woods T. E., Klessen R. S., Heger A., Whalen D. J., 2018, *MNRAS*, 474, 2757
- Hasinger G., 2020, *J. Cosmology Astropart. Phys.*, 2020, 022
- Hayes M. J. et al., 2024, *ApJ*, 971, L16
- Hirano S., Hosokawa T., Yoshida N., Kuiper R., 2017, *Science*, 357, 1375
- Hosokawa T., Omukai K., Yorke H. W., 2013, *ApJ*, 778, 178
- Hosokawa T., Yorke H. W., Inayoshi K., Omukai K., Yoshida N., 2013, *ApJ*, 778, 178
- Inayoshi K., Tanaka T. L., 2015, *MNRAS*, 450, 4350
- Inayoshi K., Visbal E., Haiman Z., 2020, *ARA&A*, 58, 27
- Jeon J., Bromm V., Liu B., Finkelstein S. L., 2024, arXiv e-prints, arXiv:2402.18773
- Jiang L. et al., 2020, *Nature Astronomy*
- Jiang Y.-F., Stone J. M., Davis S. W., 2019, *ApJ*, 880, 67
- Johnson J. L., Bromm V., 2007, *MNRAS*, 374, 1557
- Juodžbalis I. et al., 2024, arXiv e-prints, arXiv:2403.03872
- Katz H., Sijacki D., Haehnelt M. G., 2015, *MNRAS*, 451, 2352
- Kovács O. E. et al., 2024, *ApJ*, 965, L21
- Larson R. L. et al., 2023, *ApJ*, 953, L29
- Latif M. A., Ferrara A., 2016, *PASA*, 33, e051
- Latif M. A., Khochfar S., 2020, *MNRAS*, 497, 3761
- Latif M. A., Omukai K., Habouzit M., Schleicher D. R. G., Volonteri M., 2016, *ApJ*, 823, 40
- Latif M. A., Schleicher D. R. G., Schmidt W., Niemeyer J. C., 2013, *MNRAS*, 436, 2989
- Latif M. A., Whalen D. J., Khochfar S., Herrington N. P., Woods T. E., 2022, *Nature*, 607, 48
- Li J. et al., 2024, arXiv e-prints, arXiv:2403.00074
- Lupi A., Haardt F., Dotti M., Fiacconi D., Mayer L., Madau P., 2016, *MNRAS*, 456, 2993
- Lupi A., Haiman Z., Volonteri M., 2021, *MNRAS*, 503, 5046
- Lupi A., Quadri G., Volonteri M., Colpi M., Regan J. A., 2024, *A&A*, 686, A256
- Ma L., Hopkins P. F., Ma X., Anglés-Alcázar D., Faucher-Giguère C.-A., Kelley L. Z., 2021, *MNRAS*, 508, 1973

- Madua P., Rees M. J., 2001, *ApJ*, 551, L27
- Maggiore M. et al., 2020, *J. Cosmology Astropart. Phys.*, 2020, 050
- Maiolino R. et al., 2024a, arXiv e-prints, arXiv:2405.00504
- Maiolino R. et al., 2024b, *Nature*, 627, 59
- Mapelli M. et al., 2021, *MNRAS*, 505, 339
- Matthee J. et al., 2024, *ApJ*, 963, 129
- Mayer L., Capelo P. R., Zwick L., Di Matteo T., 2024, *ApJ*, 961, 76
- Mayer L., Fiacconi D., Bonoli S., Quinn T., Roškar R., Shen S., Wadsley J., 2015, *ApJ*, 810, 51
- Mayer L., Kazantzidis S., Escala A., Callegari S., 2010, *Nature*, 466, 1082
- Milosavljević M., Couch S. M., Bromm V., 2009, *ApJ*, 696, L146
- Mortlock D. J. et al., 2011, *Nature*, 474, 616
- Nandal D., Regan J. A., Woods T. E., Farrell E., Ekström S., Meynet G., 2023, *A&A*, 677, A155
- Natarajan P., 2020, *MNRAS*
- Natarajan P., Pacucci F., Ricarte A., Bogdán Á., Goulding A. D., Cappelluti N., 2024, *ApJ*, 960, L1
- Ni Y. et al., 2022, *MNRAS*, 513, 670
- Pacucci F., Natarajan P., Volonteri M., Cappelluti N., Urry C. M., 2017, *ApJ*, 850, L42
- Pelupessy F. I., van Elteren A., de Vries N., McMillan S. L. W., Drost N., Portegies Zwart S. F., 2013, *A&A*, 557, A84
- Pezzulli E., Valiante R., Schneider R., 2016, *MNRAS*, 458, 3047
- Pfister H., Lupi A., Capelo P. R., Volonteri M., Bellovary J. M., Dotti M., 2017, *MNRAS*, 471, 3646
- Pfister H., Volonteri M., Dubois Y., Dotti M., Colpi M., 2019, *MNRAS*, 486, 101
- Piana O., Dayal P., Volonteri M., Choudhury T. R., 2020, *MNRAS*
- Portegies Zwart S. et al., 2009, *New A*, 14, 369
- Portegies Zwart S. F., Baumgardt H., Hut P., Makino J., McMillan S. L. W., 2004, *Nature*, 428, 724
- Prole L. R., Regan J. A., Glover S. C. O., Klessen R. S., Priestley F. D., Clark P. C., 2024, *A&A*, 685, A31
- Rantala A., Naab T., Lahén N., 2024, *MNRAS*, 531, 3770
- Regan J. A., Downes T. P., 2018, *MNRAS*, 478, 5037
- Regan J. A., Haiman Z., Wise J. H., O’Shea B. W., Norman M. L., 2020a, *The Open Journal of Astrophysics*, 3, E9
- Regan J. A., Visbal E., Wise J. H., Haiman Z., Johansson P. H., Bryan G. L., 2017, *Nature Astronomy*, 1, 0075
- Regan J. A., Wise J. H., O’Shea B. W., Norman M. L., 2020b, *MNRAS*, 492, 3021
- Regan J. A., Wise J. H., Woods T. E., Downes T. P., O’Shea B. W., Norman M. L., 2020c, *The Open Journal of Astrophysics*, 3, 15
- Reinoso B., Klessen R. S., Schleicher D., Glover S. C. O., Solar P., 2023, *MNRAS*
- Ricarte A., Tremmel M., Natarajan P., Quinn T., 2019, *MNRAS*, 489, 802
- Rizzuto F. P. et al., 2021, *MNRAS*, 501, 5257
- Sassano F., Schneider R., Valiante R., Inayoshi K., Chon S., Omukai K., Mayer L., Capelo P. R., 2021, *MNRAS*, 506, 613
- Sądowski A., 2009, *ApJS*, 183, 171
- Sądowski A., Lasota J.-P., Abramowicz M. A., Narayan R., 2016, *MNRAS*, 456, 3915
- Sądowski A., Narayan R., 2016, *MNRAS*, 456, 3929
- Schauer A. T. P., Glover S. C. O., Klessen R. S., Clark P., 2021, *MNRAS*, 507, 1775
- Schneider R., Salvaterra R., Ferrara A., Ciardi B., 2006, *MNRAS*, 369, 825
- Scholtz J. et al., 2023, arXiv e-prints, arXiv:2311.18731
- Sesana A., Volonteri M., Haardt F., 2007, *MNRAS*, 377, 1711
- Sesana A., Volonteri M., Haardt F., 2009, *Classical and Quantum Gravity*, 26, 094033
- Shang C., Bryan G. L., Haiman Z., 2010, *MNRAS*, 402, 1249
- Shi Y., Kremer K., Hopkins P. F., 2024
- Singh J., Monaco P., Tan J. C., 2023, *MNRAS*, 525, 969
- Smith B. D., Regan J. A., Downes T. P., Norman M. L., O’Shea B. W., Wise J. H., 2018, *MNRAS*, 480, 3762
- Spinoso D., Bonoli S., Valiante R., Schneider R., Izquierdo-Villalba D., 2023, *MNRAS*, 518, 4672
- Spolyar D., Freese K., Gondolo P., 2008, *Phys. Rev. Lett.*, 100, 051101
- Tremmel M., Karcher M., Governato F., Volonteri M., Quinn T. R., Pontzen A., Anderson L., Bellovary J., 2017, *MNRAS*, 470, 1121
- Trinca A., Schneider R., Valiante R., Graziani L., Zappacosta L., Shankar F., 2022, *MNRAS*, 511, 616
- Turk M. J., Abel T., O’Shea B., 2009, *Science*, 325, 601
- Venemans B. P. et al., 2015, *ApJ*, 801, L11
- Venemans B. P. et al., 2013, *ApJ*, 779, 24
- Visbal E., Haiman Z., Bryan G. L., 2014, *MNRAS*, 445, 1056
- Visbal E., Haiman Z., Terrazas B., Bryan G. L., Barkana R., 2014, *MNRAS*, 445, 107
- Vogelsberger M. et al., 2014, *MNRAS*, 444, 1518
- Volonteri M., Habouzit M., Colpi M., 2021, *Nature Reviews Physics*, 3, 732
- Volonteri M., Rees M. J., 2005, *ApJ*, 633, 624
- Wang F. et al., 2021, *ApJ*, 907, L1
- Whalen D., Abel T., Norman M. L., 2004, *ApJ*, 610, 14
- Wise J. H., Regan J. A., O’Shea B. W., Norman M. L., Downes T. P., Xu H., 2019, *Nature*, 566, 85
- Woods T. E., Heger A., Whalen D. J., Haemmerlé L., Klessen R. S., 2017, *ApJ*, 842, L6
- Woods T. E., Willott C. J., Regan J. A., Wise J. H., Downes T. P., Norman M. L., O’Shea B. W., 2021, *ApJ*, 920, L22
- Xu H., Wise J. H., Norman M. L., 2013, *ApJ*, 773, 83
- Yang J. et al., 2021, *ApJ*, 923, 262
- Yoshida N., Abel T., Hernquist L., Sugiyama N., 2003, *ApJ*, 592, 645
- Yue M., Eilers A.-C., Ananna T. T., Panagiotou C., Kara E., Miyaji T., 2024a, arXiv e-prints, arXiv:2404.13290
- Yue M., Eilers A.-C., Ananna T. T., Panagiotou C., Kara E., Miyaji T., 2024b, arXiv e-prints, arXiv:2404.13290
- Zubovas K., King A., 2021, *MNRAS*, 501, 4289

This paper was built using the Open Journal of Astrophysics L^AT_EX template. The OJA is a journal which

provides fast and easy peer review for new papers in the **astro-ph** section of the arXiv, making the reviewing process simpler for authors and referees alike. Learn more at <http://astro.theoj.org>.